Computational assessment of wind flow field on and around atypical buildings

Rajasekarababu KB (kb.rajasekarababu2014@vit.ac.in)
Vellore Institute of Technology Chennai

Research

Keywords: Set-back, Taper building, Rectangular building, pressure coefficients, Tall buildings, CFD, IDDES, Iso-surface

Posted Date: July 24th, 2020

DOI: https://doi.org/10.21203/rs.3.rs-45389/v1

Computational assessment of wind flow field on and around atypical buildings

KB Rajasekarababu*
Aerodynamics Laboratory School of Mechanical Engineering,
Vellore Institute of Technology Chennai -600127 INDIA.
*kb.rajasekarababu2014@vit.ac.in**

Abstract. This article provides an overview of pressure coefficients (*Cp*) on atypical tall buildings with the application of CFD. Various modifications in architectural shapes on tall buildings eventually lead to a reduction in the wind load on building surfaces. The surface pressure on conventional (Square and rectangular) buildings is relatively different in comparison to other tall buildings. This study is to evaluate the surface pressure coefficient over rectangular, taper and setback buildings. The computational results show that the taper building has 7% *Cp* rise at ground level (*y/H*=0.225) in the windward face, and 34% *Cp* fall at the middle level (*y/H*=0.475) in the side face when compared with the rectangular building. Whereas for the setback building, *Cp* at ground level near setback (*y/H*=0.225) has reduced to about 25% and about 6% at the middle level (*y/H*=0.475) in windward than that in the rectangle building. Also, the side faces of the setback showed a 15% drop in Cp than other buildings. In leeward face, *Cp* is reduced to 56% near setback at the top of the building (*y/H*=0.725). This valuation of the *Cp* on these buildings shows that the effect of setbacks on building reduces the pressure variation on all faces and the downstream wake vortices.

Keywords: Set-back; Taper building; Rectangular building; pressure coefficients; Tall buildings; CFD; IDDES and Iso-surface.

1 Introduction

In developed countries, there is an extensive emergence of tall structures. They are highly sensitive to the action of wind force which is a demanding task for the structural engineers and architects in connection with habitability, serviceability, and survivability. And the assurance of essential structural performance also becomes difficult to vindicate. The influence of strong wind excitation intensity on tall buildings is effectively felt on adjacent buildings and wind environments outdoor. It inevitably affects wind acceleration at the ground level, wind noise, vegetation and the comfort of the pedestrian. Wind tunnel testing and field investigations are the two notable methods used to explore and study the wind flows. Both the assessments are costly and time- consuming.

An alternative as well as a redundant tool to study and investigate wind loads on buildings in recent times, is CFD (Computational Fluid Dynamics). CFD can be referred to as a virtual wind tunnel in wind engineering which is capable of generating environmental flows to predict the flow physics. The CFD procedures in wind engineering studies has recognized a plethora of importance from several international engineering communities. It has motivated the establishment of CFD practice guidelines by Franke et al. [1&2], Tominaga, Y [3] and Blocken et al. [4]. 3D RANS model approach was used by various researchers in the past to study wind flow around buildings (Jian Hang et al. [5], W.D.Janssen [6], Jianlin Liu and Jianlei Niu [7], Blocken et al. [8], K.T. Tse et al. [9]). H. Tanaka et al. [10] presented the flow features like pressure coefficients, overturning moment coefficients and PSD (Power Spectral Density) on and around aerodynamically modified tall buildings using numerical and experimental results. From the experimental analysis of suburban and open terrain wind flow, Yong Chul Kim & Jun Kanda [11] concluded that the set-backed models are more practical to reduce the fluctuating lift force than the tapered or square models. Later, time-domain and frequency-domain analysis were performed by Yong Chul Kim [12] on a square,

tapered and setback models with the side ratio of 1:1. A lot of unconventional building studies are being carried out. Yong Chul Kim et al. [13] examined the wind-induced coupled motion on plan varying tall buildings vs square buildings and found that the along-wind and torsional accelerations are smaller in the first. Using DDES (Delayed Detached Eddy Simulation) and IDDES (Improved Delayed Detached Eddy Simulation) turbulence models, Rajasekarababu et al. [14] explored the velocity profiles, upstream stagnation, and surface pressure distribution around a setback building. They concluded that DDES under predicted the downstream recirculation compared with IDDES turbulence model. Concerning recent literature studies, complex time-varying 3D wind flow field on and around the buildings have been estimated accurately with the support of IDDES turbulence model in CFD techniques.

The following section generally outlines several computational parameters that may affect both the accuracy and efficiency of computational simulation, such as the computational domain and its setting parameters. Meanwhile, pressure coefficients assessed in four different heights (y/H=0.225, 0.475, 0.725 and 0.975 respectively) are shown in fig1. ANSYS Fluent 18 is used to perform the CFD simulation, and IDDES turbulence model is used to assure the validity and reliability of this computational assessment. Section 3 comprehensively compared wind pressure coefficients on and around tall buildings throughout their perimeter. Overall, the outcome of this assessment is to enlighten the engineers and architects with a elementary understanding of tall buildings. It helps to study indoor and outdoor natural ventilation environments.

2 Methodology

2.1 Model Description and Computational Parameter settings

This work considered a setback building of 210 m full scale height with side ratio 1:1.5 and roof–floor to base -floor area ratio 1:6.25 with a roof and three setbacks. The geometric scale chosen in the wind tunnel experiment is 1/300 for the open terrain environmental wind flow. The longer building face is 0. 015m, and the shorter face is 0.01m (D). H is the total height of the model, which is taken as 7D (H is same for all buildings); base floor area is 0.15m x 0. 1m and subsequent setbacks in higher floors are d' =D/1.25, d" =D/1.66 and d’’’=D/2.5. For the rectangular building, roof dimension is same as that of base floor dimension and for taper building roof dimension, d=D/2.5 and is as shown in Fig.1(a) (For all building the base floor dimensions are the same (0.15m x 0. 1m)). The grid distribution was done in ANSYS ICEM CFD for the 3 buildings is shown in Fig.1 (b). A grid independence test was done, which includes a comparison of results from grids of various factors like, first wall distance, stretching ratio and density. The refined grid for rect, taper and setback buildings is 8.9, 8.2, 8.7 million cells respectively. Further, the solver settings are performed on ANSYS FLUENT 18.0 with SIMPLE (Semi-Implicit Method for Pressure-Linked Equations) pressure-velocity coupling algorithm. With the combination of Shear Stress Transport, 3-D unsteady RANS equation is solved in IDDES following Rajasekarababu et al., [15]. For spatial discretization in the pressure-based solver, Least Square Cell-Based method was used as gradient, and the second-order scheme was chosen for pressure. The second-order upwind scheme is used for turbulent kinetic energy and turbulent dissipation rate terms. Bounded Central Differencing for momentum and transient formulation second-order implicit was used in the numerical methods. The convergence is assumed to be achieved when all the scaled residuals are levelled off and when the XYZ momentum, K, ω and continuity are set to at least 10^{-5}. Whereas, the time step size is (Δt=Typical cell size / Characteristic flow mean velocity) Δt= 0.00014. The assumed residuals of the computational simulation were achieved and monitored over a considerable period.

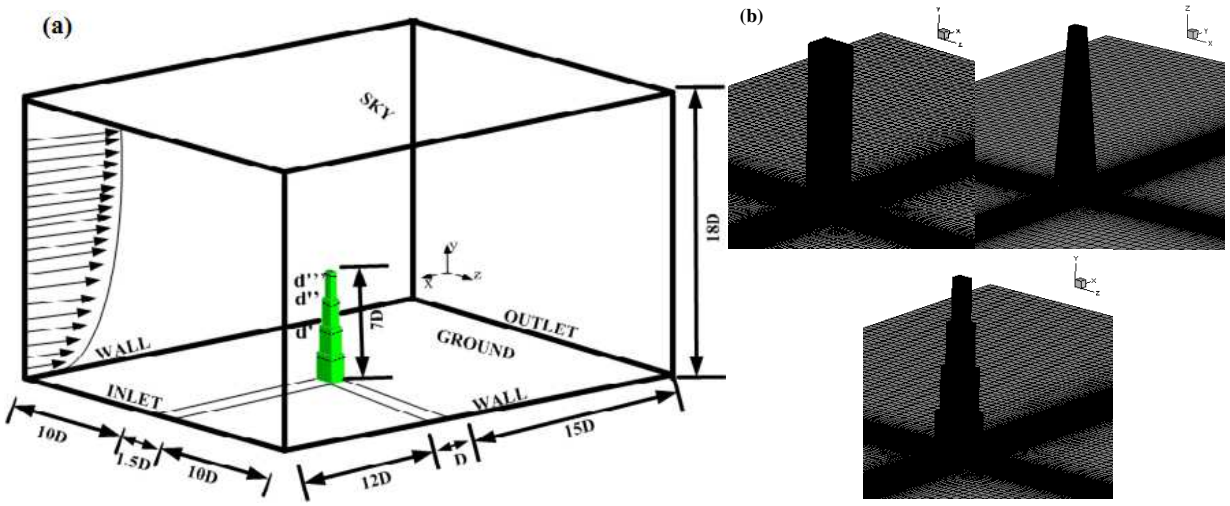

Fig.1. Perspective views on (a) computational domain and building (b) Grid distribution (Fine).

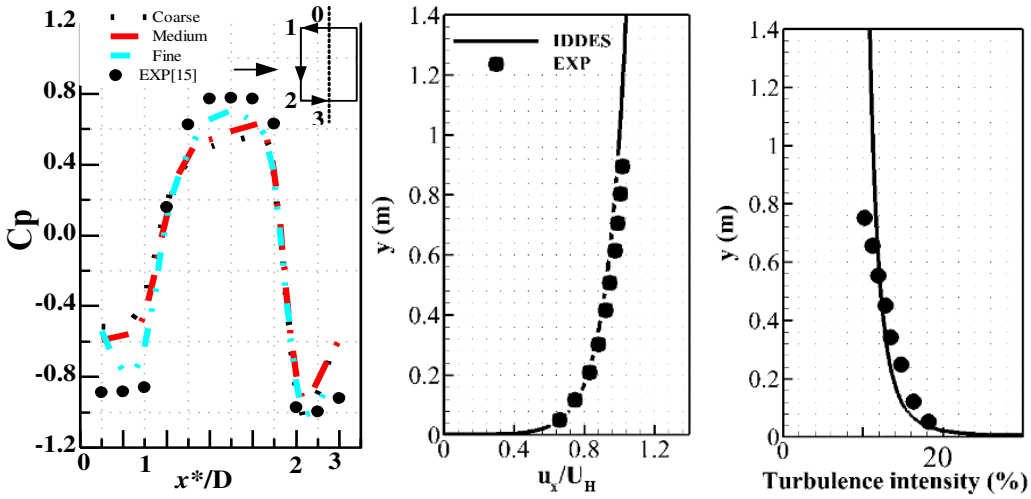

Fig.2. (a) Grid independence comparison (b) Inlet velocity and (c) Turbulence intensity profiles

The grid independence results are shown in Fig.2 (a) using the simulated and measured Cp values along half the perimeter of the setback building (x*/D) at y/H =0.625. The fine grid shows good results compared to the other two grids. In the grid independence test, it was challenging to accurately reproduce the negative pressure zone on building side face due to the viscous stress and high velocity of the bulk flow in the separation zone. The open terrain ABL profiles are simulated at a mean wind speed (U_{mean}) of 13.6 m/s and turbulent intensity of 11% are shown in Fig.2 (b &c).

Table.1 Inflow boundary conditions

Inflow conditions	
Inflow boundary (Inlet)	$(U_y) = \frac{u_{ABL}*}{\kappa}\ln\left(\frac{y+y_o}{y_o}\right); \varepsilon(y) = \frac{u*^3}{\kappa(y+y_0)}; \omega(y) = \frac{\varepsilon(y)}{C\mu k(y)}$
Outlet	$\frac{\partial}{\partial x}(U,V,W,k,\omega) = 0 \ \ (\mathrm{Pr}essure - outlet)$
Sky (top)	$U = U_{ABL}, k = k_{ABL,}\omega = \omega_{ABL},$ $W = 0, \frac{\partial}{\partial x}(U,V,W,k,\omega) = 0$
Wall (sidewall)	$V = 0, \frac{\partial}{\partial x}(U,V,W,k,\omega) = 0$
Ground wall	$K_S = \frac{9.793 y_0}{C_s}$

3 Results and Discussion

3.1 The Pressure coefficient (*Cp*) on the tall building:

The below-given equation used to calculate the pressure coefficient (*Cp*).

$$C_p = \frac{p - p_0}{\frac{1}{2}\rho U_H^2} \qquad (1)$$

Where *p* denotes is the extracted pressure from the required height. p_0 is the static pressure at the reference height, ρ indicates the density of air (1.225 Kg/m^3), U^2_H is the mean wind velocity at the building's reference height. The pressure coefficients are measured below 10% of each setback height (see d, d', d" in Fig.1). The pressure coefficient extracted at three different heights on the building are compared and are shown in Fig.3. The assessed pressure coefficient on taper and setback building are compared with rectangular (rect) building. In the windward face, taper building experienced high pressure compared with rect building and increased 3% at *y/H*=0.225. In contrast, setback *Cp* fell 21% at the same height. In the windward face, at *y/H*=0.475, both tapered and rect building showed the same positive pressure whereas at *y/H* = 0.725 taper building showed a 7% increase concerning rect building. Similarly, setback windward face at the corresponding heights mentioned before falls by 4% and 17% respectively. The *Cp* for windward face is positive, and the windward edges experienced negative *Cp* due to wind shear. The side face of the building experienced fluctuating pressure due to strong shear wind force on its leading edges. The pressure in the right side face reduced by 11%, at the same time, there was a sudden pressure fall of 32% in the leeward side when compared with rect building at *y/H*=0.225 for both taper and setback. The *Cp* in the right side face of taper and the setback building were seen reduced by 5% and 12% respectively at *y/H*=0.475. At the

same instance, there is a dramatic reduction of 51% in the leeward face for setback and just 16% for taper. Left side face of the taper and setback building was observed to be reduced by 12% and 32% respectively. The wind profile exponentially showed changing along with height; the increase of wind velocity influences the wind flow around the building. The pressure coefficients on the edges of the rect building at y/H=0.725 observed a considerable drop, as shown in Fig.3. (c). Shows that a huge suction created on the side faces. Similarly, a large fluctuation was noticed in the leeward face, which indicates the vortex formation. Furthermore, at y/H=0.725 on the right side face of the taper and setback building, Cp decreased by 70% and 90% respectively. Moreover, there is also a 54% and 82% reduction of Cp on the left side faces of the taper and setback buildings respectively. At y/H=0.975, taper and rect buildings evidenced vortex shedding and wake formation in downstream; as a result, the pressure drops on the leeward face as shown in Fig.3. (d)

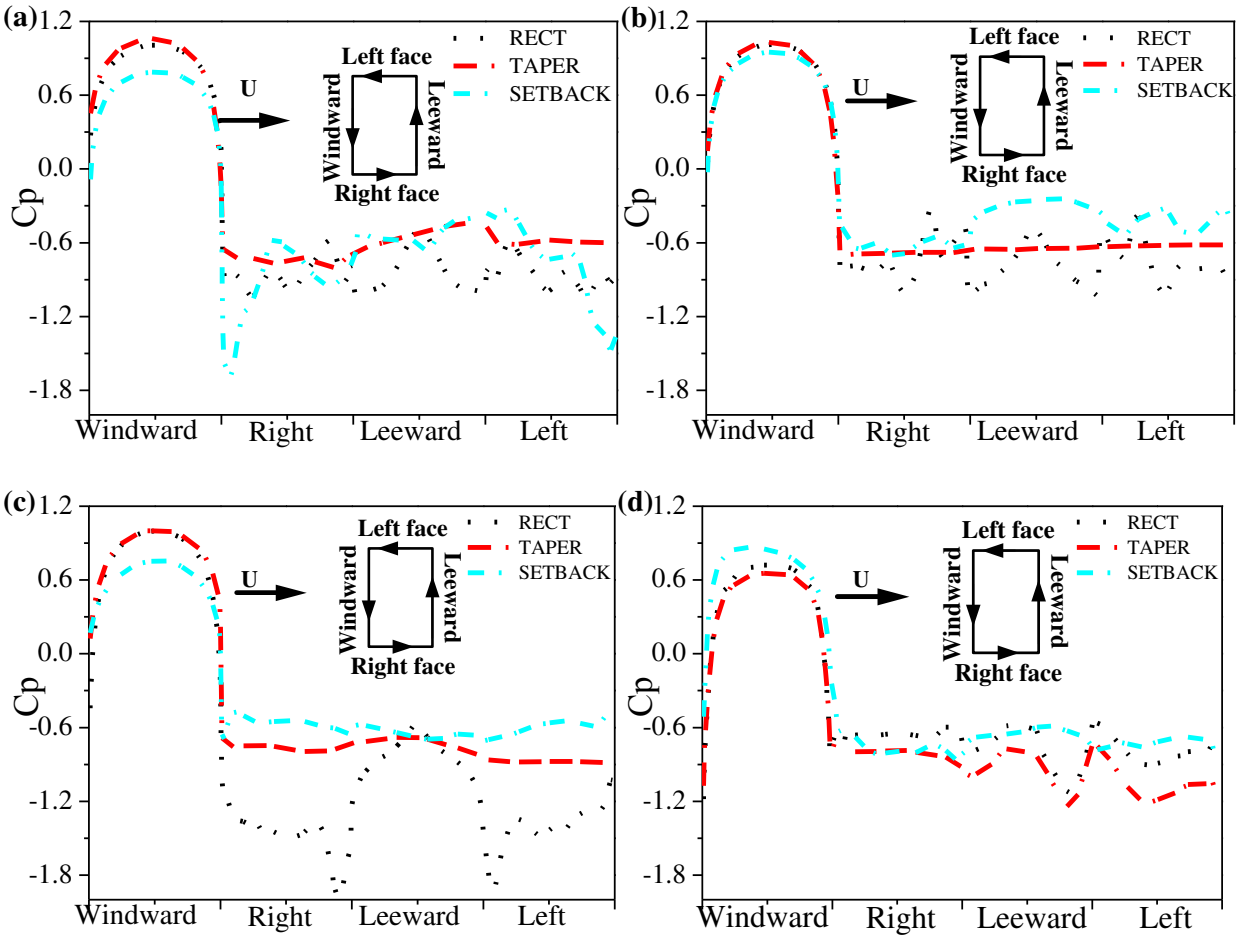

Fig.3 Pressure coefficients on buildings at 4 different heights (a) y/H=0.225, (b) 0.475,(c) 0.725 and (d) 0.975.

The pressure distribution on each side of the building shown in Fig.4. For rect building Cp= - 2.2 is the maximum negative pressure on the top face (roof), which depicted in Fig.4 (a), the strong upwind shear layer creates the cavity zone on the roof of the rect building which leads to recirculation. In Fig.4 (b) and (c) taper and setback roof has maximum negative Cp of -1.2 and -0.8 respectively, this shows

modifications along with the height of the building, and there is also moderations in the wind loads on roof, thereby decreasing the recirculation on roofs.

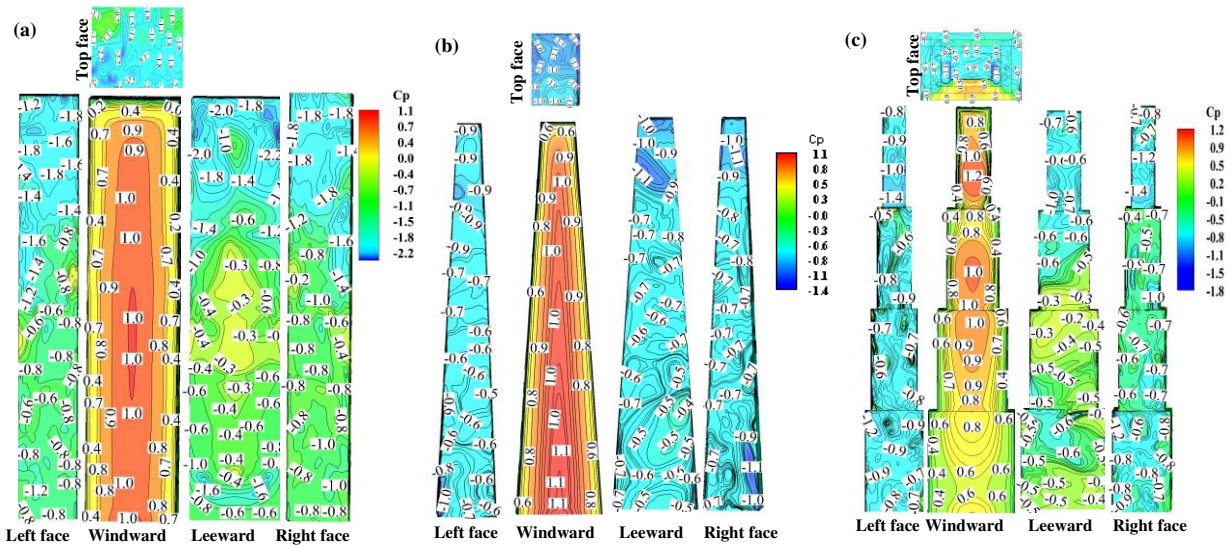

Figure 4: The distribution of Pressure coefficients on building face (a) Rectangle, (b) Taper & (c) Setback

3.2 Instantaneous vortex structure formation around buildings:

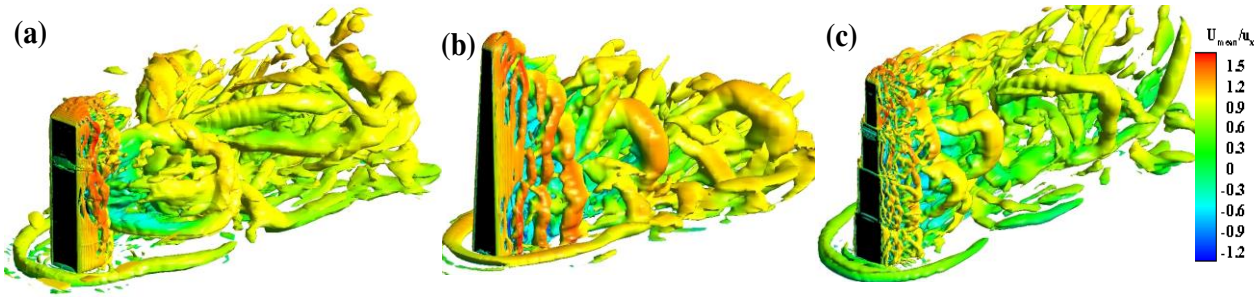

Fig. 5 Instantaneous vortex structure around buildings (Isosurface of velocity (Q= 750 ms^{-1})) (a) Rectangle, (b) Taper & (c) Setback.

The vortex formations on buildings are visualized in CFD to compare the vortex structures behind them; a Q-criterion used to identify the wake vortices using Eq. (2).

$$Q = \frac{1}{2}\left(r_{ij}r_{ij} - s_{ij}s_{ij}\right) \qquad (2)$$

Isosurface Q- criterion with non-dimensional velocity contour is used to obtain the preferred large eddy flow structure (excluding small-scale vortices of no interest). The instantaneous vortex structures identified behind the building (with Q=750) by IDDES turbulence model using fine mesh are shown in Fig.4. This indicates the capability of the simulation to solve turbulence by providing shielding function for the SST-based IDDES model in order to achieve highly chaotic large and small scale vortices. The IDDES captures the vastly separated flow of 3D stream wise and transverse vertical structures. This flow structure reveals the streams behind the unconventional building physics, especially in the sides of the separation and wake regions. The visualization of vortices indicates the intensity of the turbulence downstream for the buildings. The upstream horseshoe (HS) vortex in the windward face of the rect building has been compared with the other two buildings. At the same time, the trailing vortex structure in rect building has an un-symmetrical wake region which shows the presence of a wake oscillation with lower frequency. This phenomenon opposes the higher frequency vortex shedding with higher energy turbulence which is shown in Fig.5 (a). In taper building, the area of the wake region reduces along with the height (like a wake funnel as in Fig.5 (b)). The trailing wake regions in the setback building differs from the other two buildings as the setbacks on building break the vortices into small parts which eventually slows down the downstream driving parts. Moreover, it reduces the vortex stretching in downstream, sees Fig.5 (c). Simultaneously, the permanently attached upstream edge vortices in windward face and roof of the setbacks are relatively smaller compared to the rest of the buildings.

3.3 Comparison of Turbulence Intensity around the buildings:

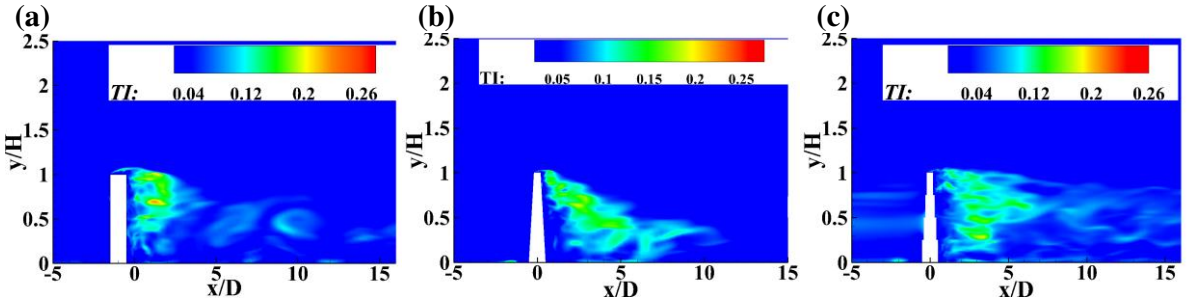

Fig. 6 Turbulence intensity around buildings (a) Rectangle, (b) Taper & (c) Setback.

Turbulence Intensity (TI) contour for three buildings is presented in Fig.6. The TI changes along with the height in the wake zone. Regarding the intensity of the turbulence on rect building, the maximum intensity is located in the recirculation region due to viscous shear separated from the leading edge. In taper, the roof leading edge shear stress influences intensely in downstream wake zone (Fig.6 (b)) and the TI core extended up to 5D. The presence of set-backs design on building breaks the core intensity of the turbulence substantially and dissipates into small eddies in downstream. (Fig.6 (c)).

3.4 Comparison of Aerodynamic force coefficients :

For the wind-induced building response analysis, the aerodynamic force coefficients are crucial. Similarly, the lift force coefficients have significant effects on the background and resonant responses of the tall buildings. The mean aerodynamic force coefficients calculated by using Eq. (3) and (4), which are functions of approached wind flow.

$$C_d = \frac{F_D}{\frac{1}{2}\rho U_H^2 D} \quad (3)$$

$$C_l = \frac{F_L}{\frac{1}{2}\rho U_H^2 D} \quad (4)$$

Where C_d and C_l are the drag and lift force coefficients, F_D is the streamwise wind force, F_L is the transverse wind force, and U^2_H is the reference velocity at the measured height and D is the projected width parallel to the wind direction. Fig.7. Shows the comparison of aerodynamic force coefficients of the buildings.

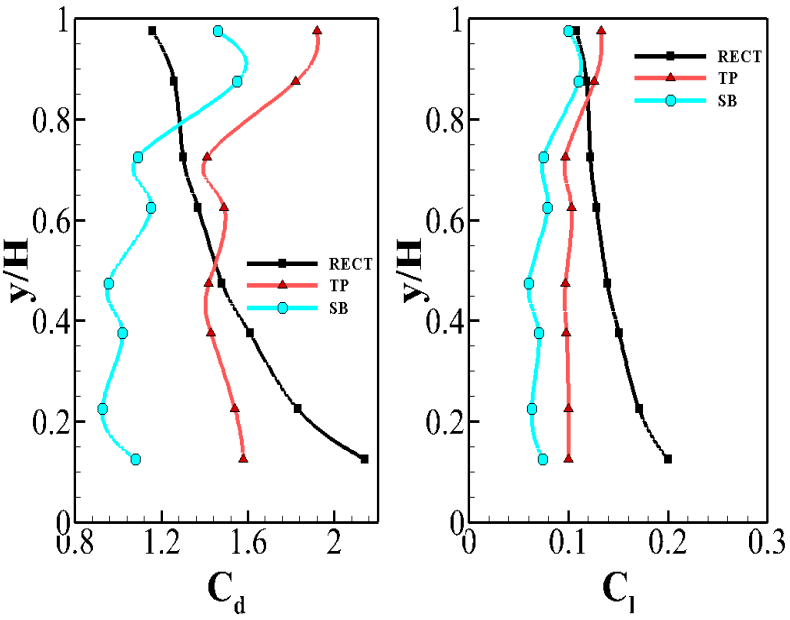

Fig. 7 Aerodynamic coefficient of atypical buildings (a) C_d, (b) C_l

The aerodynamic coefficients are measured at 8 different heights and all the aerodynamic coeffcient curves varied with height. Especially in setback building C_d values reduced near the setback due to flow break down. In rect building, the value of C_d is high nearly 2.3 at ground level, and it reduces along with height as seen in Fig.7. Furthermore, taper building C_d value is high at 8th level (y/H=0.975), which is quite close to 0.9H measured by Kim et al., [16] in their wind tunnel testing. The main cause of these drag variation along the height is due to variation in wind pressure distribution on the leeward face as a result of the characteristics of geometric shapes of the building. The advantage of height modification in tall buildings is that, as a downdraft is suppressed on account of increasing the width with low wind speed (ground level wind) and an up-flow is accelerated on account of increasing width with high wind speed, the height variation of leeward distribution is large, which also influence on the drag force coefficients which is shown in Fig.7 (a). It is also noted that the lift coefficient (across wind force) values also show that setback and taper building is effective in across winds compare to rect building.

4 Conclusion

The purpose of this study is to assess and compare the wind flow features around conventional (rectangle) tall building over un-conventional (taper and setback) buildings using IDDES turbulence model. The substantial recommendations of this study derive the following conclusions.

- At y/H=0.475, presence of setback on the building along with height shows 51% Cp reduction and just 16% for taper in comparison with rect building for the leeward face. This is because the setbacks slow down the downstream.
- Dimensional changes along the height of the building showed a reduction of 70 and 90 percentage in Cp on the right side face of the taper and setback buildings at y/H=0.725. Moreover, there is a 54% and 82% reduction in Cp on the left side faces of both the buildings respectively.
- Instantaneous vortex structure indicates the formation of hairpin vortices with high energy at downstream due to the driving and lagging vortices. Due to largely expanded wakes, wake regions in the taper building was observed falling along with the height.
- The features of trailing vortices of setback building differ from other buildings due to downstream vortex breaks down, stretching of vortices reduced by the setbacks and the intensity of the turbulence also reduces along with the height.
- The reduction of drag coefficient is mainly initiated from the leeward pressure distribution.

Overall, from this assessment, setbacks on building reduce the wind load and ensure comfort compared with conventional tall buildings. Also, IDDES turbulence model can enumerate detailed complex flow features with limited grid spacing.

Abbreviations:

ABL Atmospheric Boundary Layer
CFD Computational Fluid Dynamics
C_d Coefficient of drag
C_l Coefficient of lift
Cp pressure coefficient
Cs Constant roughness height
D Width of the building
DDES Delayed Detached Eddy Simulation
F_D Force in the stream wise direction
F_L Force in transverse wise direction
H Height of the building
IDDES Improved Delayed Detached Eddy Simulation
I Turbulence Intensity
k Turbulence Kinetic Energy
K_s Sand grain roughness height
PSD Power Spectral Density
p Pressure
RANS Reynolds–Averaged Navier-Stokes
Rect Rectangular Building
SST Shear Stress Transport
SB Setback building
TP Taper building
URANS Unsteady RANS
U_{mena} Mean inlet velocity
U_H Velocity at the reference height
u^*_{ABL} Frictional velocity of ABL
y Max. height in the y-direction
y_o Roughness length
ε Dissipation of turbulence energy
κ Karman constant
ρ Density
ω Specific dissipation rate

Acknowledgements

Authors would like to thank all reviewers who provided valuable feedback comments.

Authors' contributions

Sole contributors to this article. The authors read and approved the final manuscript.

Funding

No funding.

Availability of data and materials

CFD simulation and wind tunnel data is available upon request.

Competing interests

The authors have no competing interest.

Author details

KB Rajasekarababu,

Aerodynamics Laboratory

School of Mechanical Engineering,

Vellore Institute of Technology Chennai -600127 INDIA.

References

[1] Franke J, editor. Best practice guideline for the CFD simulation of flows in the urban environment. Meteorological Inst.; 2007.

[2] Franke, Jorg, et al. "The COST 732 Best Practice Guideline for CFD simulation of flows in the urban environment: a summary." International Journal of Environment and Pollution 44.1-4 (2011): 419-427.

[3] Tominaga, Yoshihide, and Ted Stathopoulos. "Numerical simulation of dispersion around an isolated cubic building: model evaluation of RANS and LES." Building and Environment 45.10 (2010): 2231-2239.

[4] Blocken, Bert, Ted Stathopoulos, and Jan Carmeliet. "CFD simulation of the atmospheric boundary layer: wall function problems." Atmospheric environment 41.2 (2007): 238-252.

[5] Hang, Jian, et al. "The influence of building height variability on pollutant dispersion and pedestrian ventilation in idealized high-rise urban areas." Building and Environment 56 (2012): 346-360.

[6] Janssen, Wendy D., Bert Blocken, and Twan van Hooff. "Computational evaluation of pedestrian wind comfort and wind safety around a high-rise building in an urban area." (2014).

[7] Liu, Jianlin, and Jianlei Niu. "CFD simulation of the wind environment around an isolated high-rise building: An evaluation of SRANS, LES and DES models." Building and Environment 96 (2016): 91-106.

[8] Blocken, Bert, Ted Stathopoulos, and J. P. A. J. Van Beeck. "Pedestrian-level wind conditions around buildings: Review of wind-tunnel and CFD techniques and their accuracy for wind comfort assessment." Building and Environment 100 (2016): 50-81.

[9] Tse, Kam-Tim, et al. "Pedestrian-level wind environment around isolated buildings under the influence of twisted wind flows." Journal of Wind Engineering and Industrial Aerodynamics 162 (2017): 12-23.

[10] Tanaka, Hideyuki, et al. "Experimental investigation of aerodynamic forces and wind pressures acting on tall buildings with various unconventional configurations." Journal of Wind Engineering and Industrial Aerodynamics 107 (2012): 179-191.

[11] Kim, Yong Chul, and Jun Kanda. "Characteristics of aerodynamic forces and pressures on square plan buildings with height variations." Journal of Wind Engineering and Industrial Aerodynamics 98.8-9 (2010): 449-465.

[12] Kim, Yong Chul, Jun Kanda, and Yukio Tamura. "Wind-induced coupled motion of tall buildings with varying square plan with height." Journal of Wind Engineering and Industrial Aerodynamics 99.5 (2011): 638-650.
[13] Kim, Yong Chul, and Jun Kanda. "Wind pressures on tapered and setback tall buildings." Journal of Fluids and Structures 39 (2013): 306-321.
[14] Rajasekarababu, K. B., and G. Vinayagamurthy. "Experimental and Computational Simulation of an Open Terrain Wind Flow around a Setback Building using Hybrid Turbulence Models." Journal of Applied Fluid Mechanics 12.1 (2019).
[15] Rajasekarababu, K. B., G. Vinayagamurthy, and S. Selvi Rajan. "Experimental and computational investigation of outdoor wind flow around a setback building." Building Simulation. Vol. 12. No. 5. Tsinghua University Press, 2019.
[16] Kim, Yongchul, and Jun Kanda. "Characteristics of aerodynamic forces and pressures on square plan buildings with height variations." *Journal of Wind Engineering and Industrial Aerodynamics* 98.8-9 (2010): 449-465.

Figures

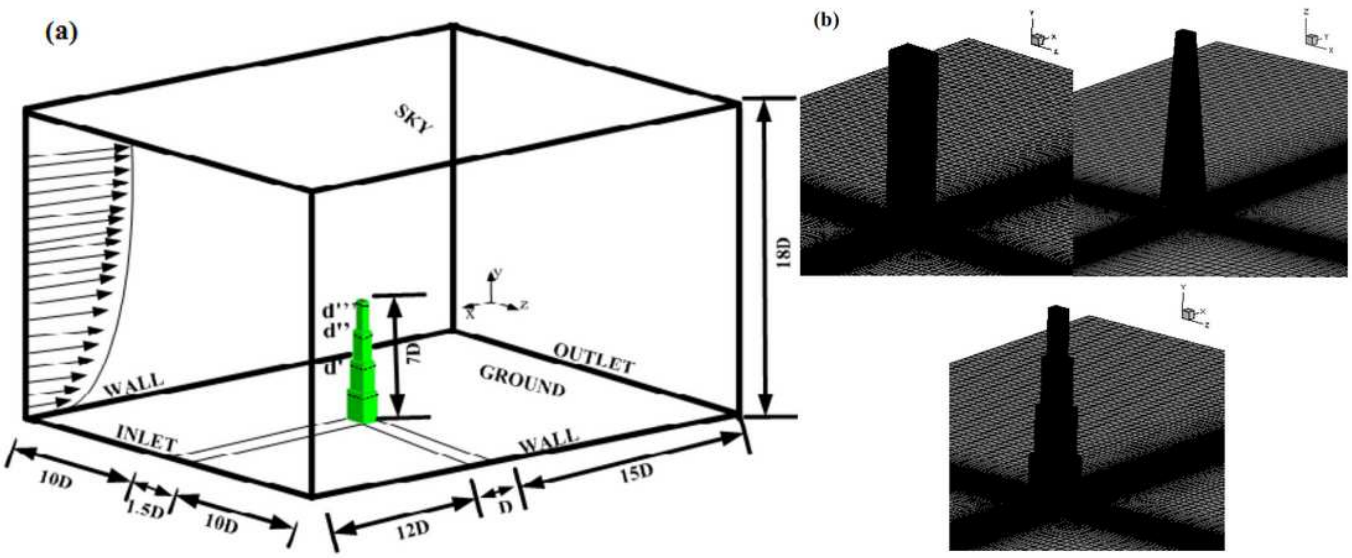

Figure 1

Perspective views on (a) computational domain and building (b) Grid distribution (Fine).

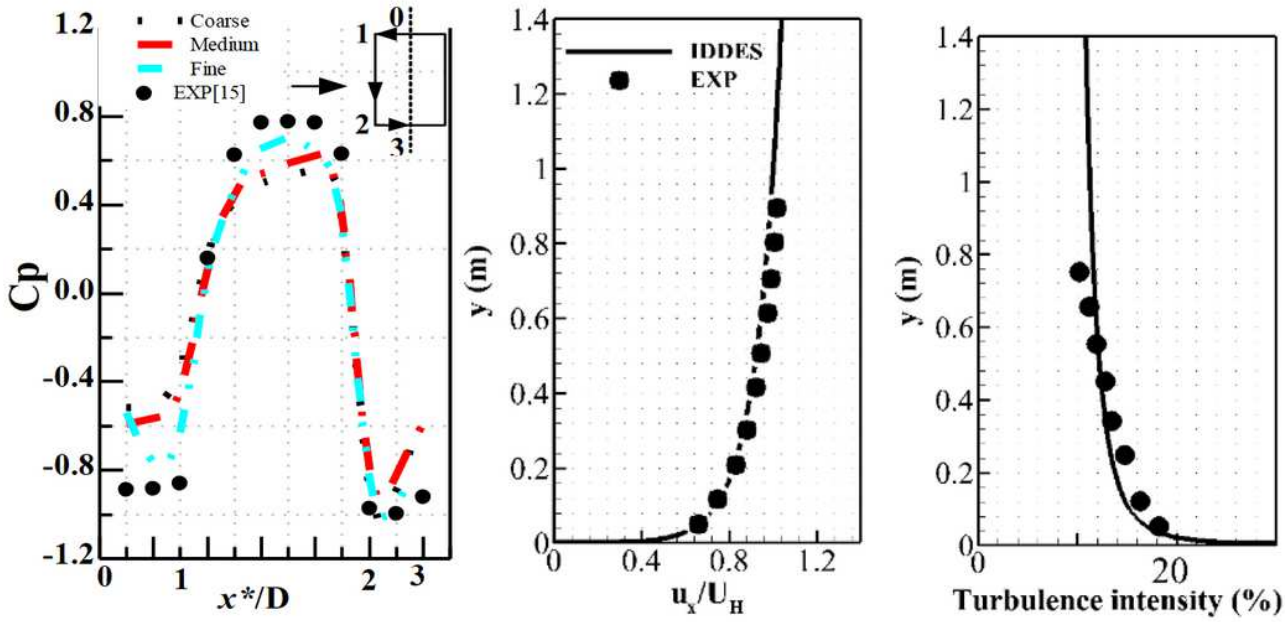

Figure 2

(a) Grid independence comparison (b) Inlet velocity and (c) Turbulence intensity profiles

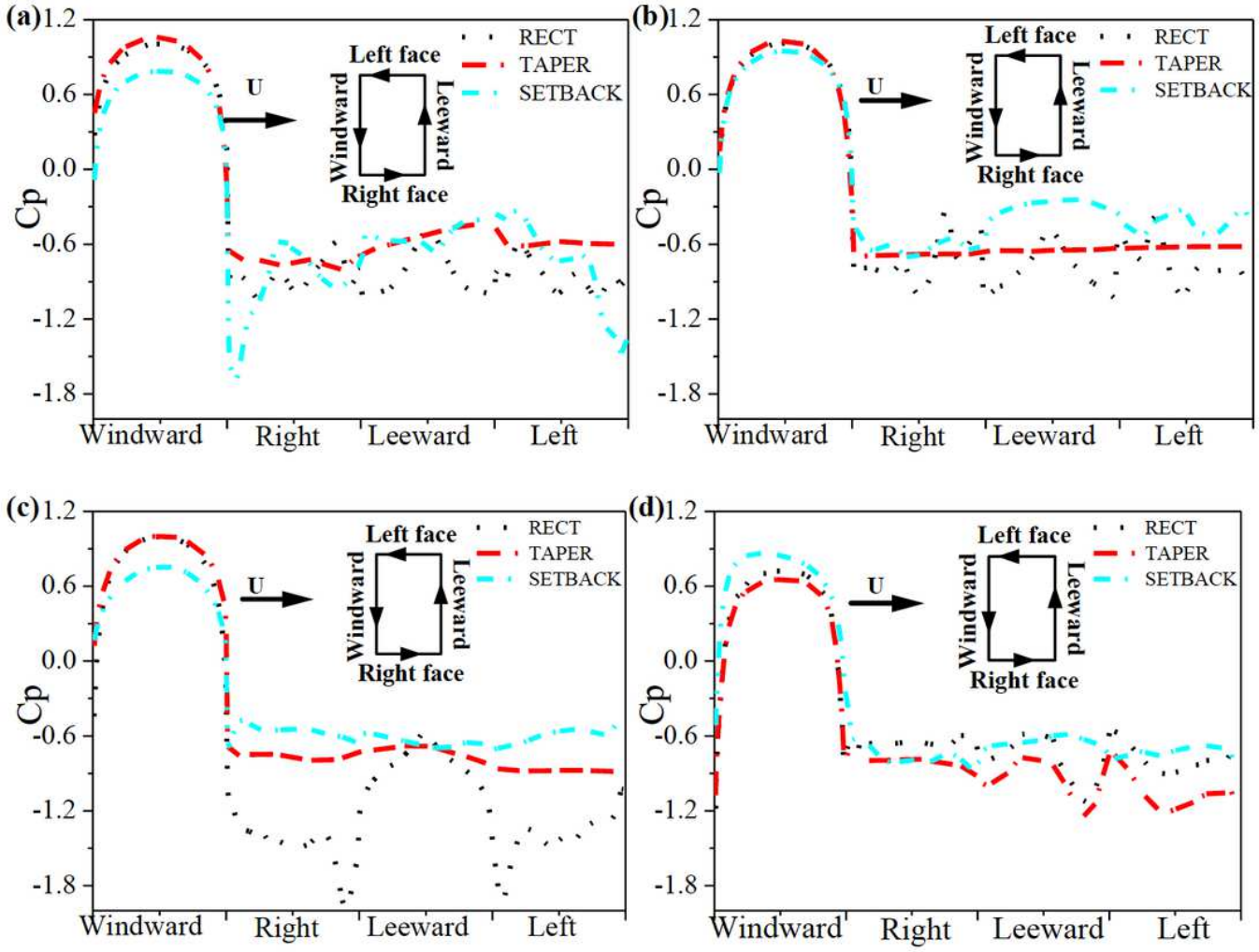

Figure 3

Pressure coefficients on buildings at 4 different heights (a) y/H=0.225, (b) 0.475,(c) 0.725 and (d) 0.975.

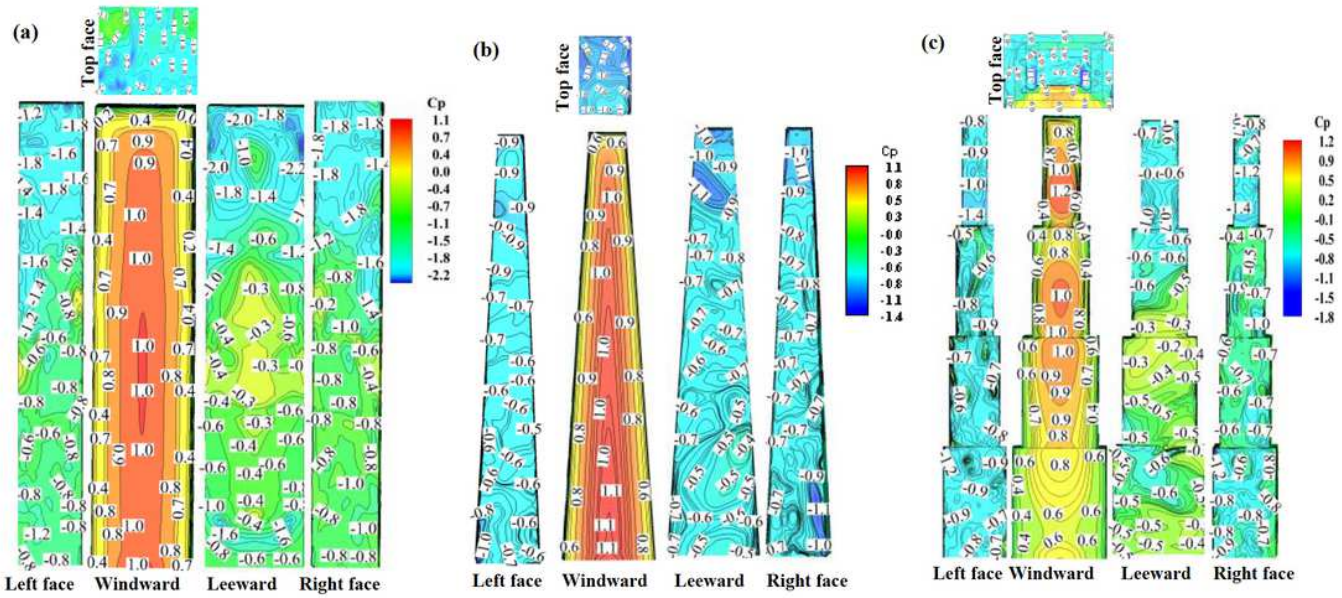

Figure 4

The distribution of Pressure coefficients on building face (a) Rectangle, (b) Taper & (c) Setback

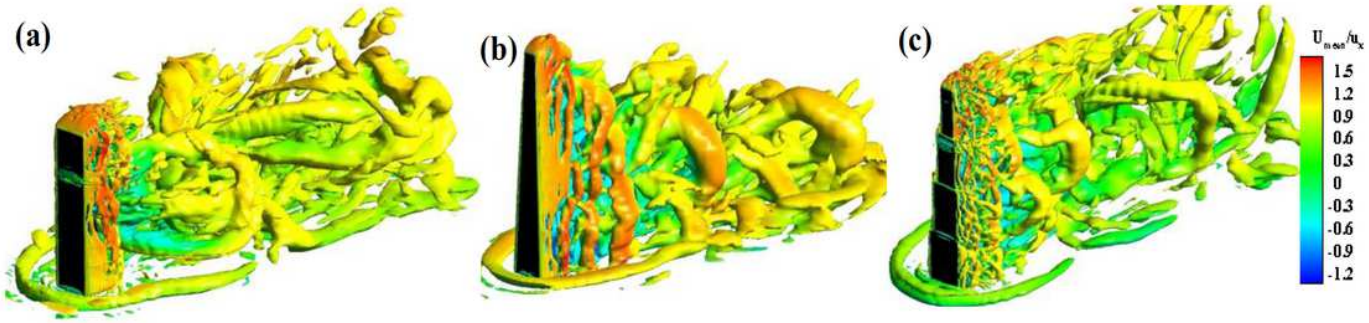

Figure 5

Instantaneous vortex structure around buildings (Isosurface of velocity (Q= 750 ms-1)) (a) Rectangle, (b) Taper & (c) Setback.

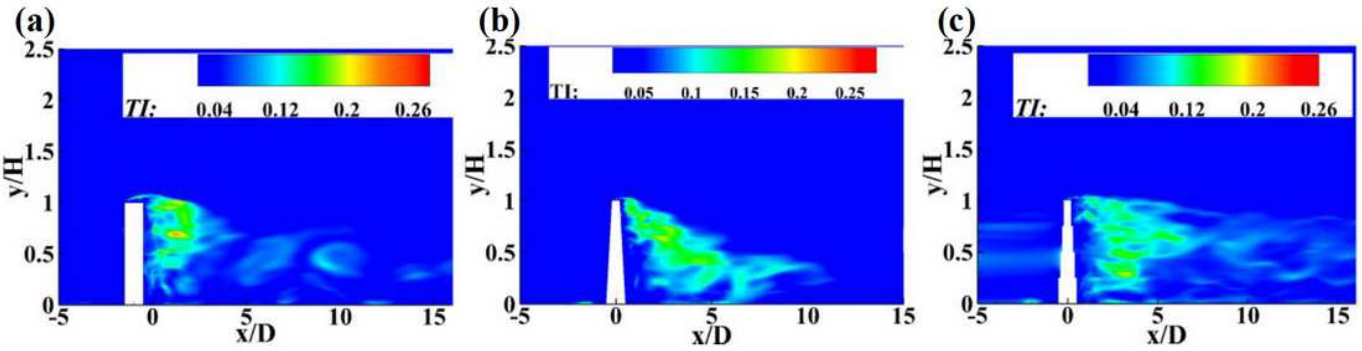

Figure 6

Turbulence intensity around buildings (a) Rectangle, (b) Taper & (c) Setback.

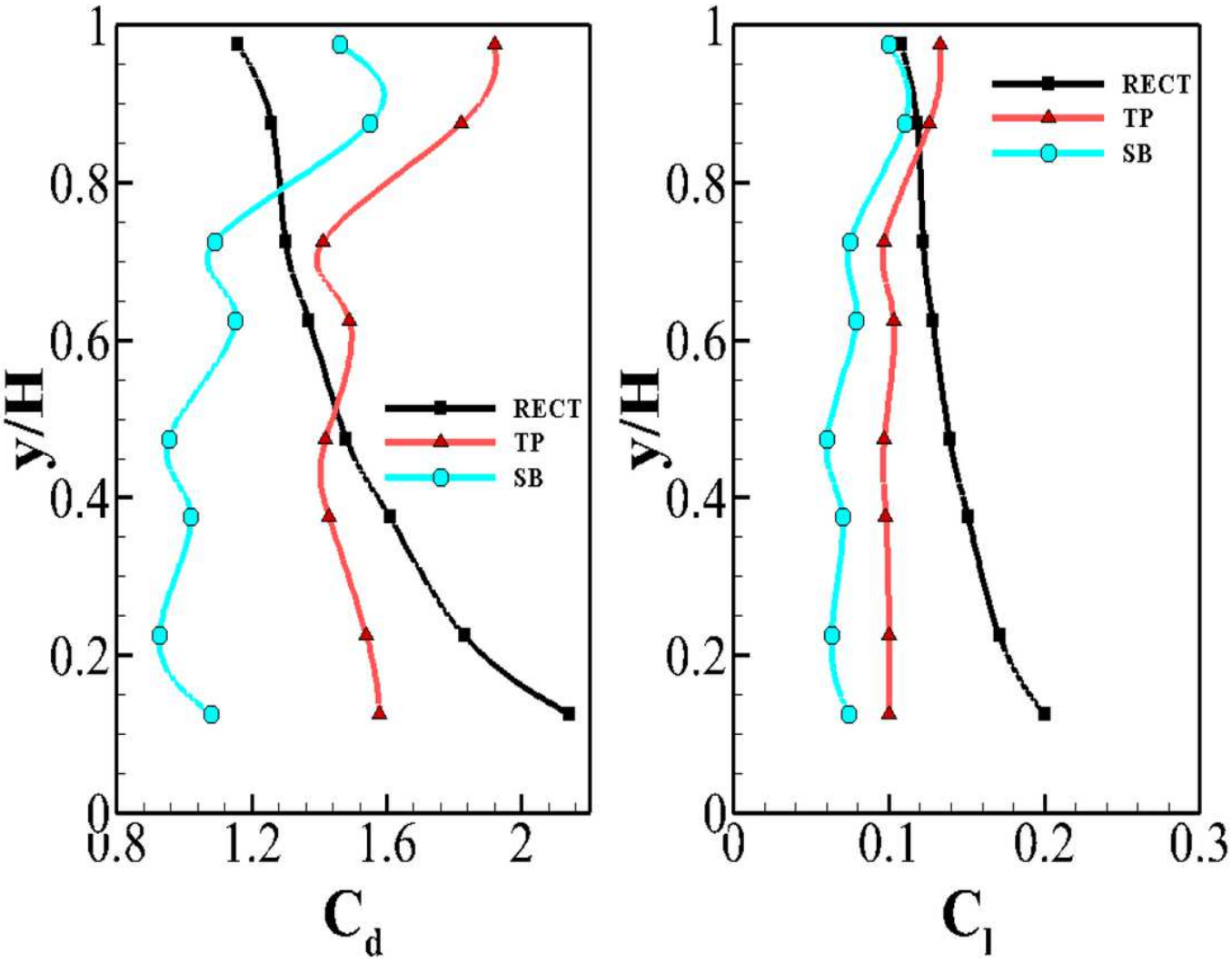

Figure 7

Aerodynamic coefficient of atypical buildings (a) Cd, (b) Cl